PROCEEDINGS of the
23rd International Congress on Acoustics
9 to 13 September 2019 in Aachen, Germany

Design of multi-directional acoustic cloaks using two-dimensional shape optimization and the boundary element method

Peter RISBY ANDERSEN(1), Vicente CUTANDA HENRÍQUEZ(2), Lorenzo SANCHIS(3), José SÁNCHEZ-DEHESA(4)

(1)Centre for Acoustic-Mechanical Micro Systems, Technical University of Denmark, Denmark, prand@elektro.dtu.dk
(2)Centre for Acoustic-Mechanical Micro Systems, Technical University of Denmark, Denmark, vcuhe@elektro.dtu.dk
(3)Wave Phenomena Group, Dep. Electronic Engineering, Universitat Politècnica de València, Spain, lorenzo.sanchis@uv.es
(4)Wave Phenomena Group, Dep. Electronic Engineering, Universitat Politècnica de València, Spain, jsdehesa@upv.es

Abstract
Acoustic cloaking is a technique that seeks hiding objects in a sound field by reducing or cancelling their scattered sound pressure. Incident waves are restored to as close as possible their original undisturbed form after hitting the cloaked object. One technique for achieving this goal is the design of additional scatterers around the object, which, properly distributed and shaped, can create cloaking at the design frequency. A newly developed numerical technique combining the Boundary Element Method (BEM) with shape optimization is applied in this work for two-dimensional cloaking of a cylinder. The shapes of the scatterers are optimized for the cloaking of the whole setup with waves impinging on the cylinder from several different directions. The results show a measure of the amount of cloaking depending on the direction at the range around the design frequency. The optimization results are compared with existing one-directional cloaks. The impact of visco-thermal acoustic losses in the cloaking design is also evaluated by means of a BEM implementation with losses.
Keywords: Acoustic cloaking, Boundary Element Method, Shape Optimization

1 INTRODUCTION

Designing acoustic cloaking devices by scattering cancellation posses a challenge. Especially, if the requirement is to offer a cloak that can operate with incident waves at different angles, i.e., a multi-directional cloak. In recent years, several examples of cloaking devices that are based on scattering cancellation have been proposed for one-directional cloaking [1, 2, 3], but also examples of multi-directional acoustic cloaks exist [4]. However, obtaining multi-directional acoustic cloaks with similar performance to its one-directional counterpart is a non-trivial task. In the Refs. [1, 2, 4], the cloaks are based on design methods that utilize simple shapes restricted to cylinders or Beziér scatters. Therefore, the design space is limited, meaning that finding satisfactory solutions can be cumbersome. In this paper, we will apply a newly developed shape optimization technique to the optimization of a multi-directional cloak. The shape optimization technique is applicable to both isentropic and lossy optimization and relies on the Boundary Element Method (BEM), which will allow more freedom for the creation of the scatter shapes [5, 6].

In the following, firstly the BEM for scatting problems is introduced, hereafter, the initial design proposal and parametrization of the multi-directional cloak is shown. This is followed by a section on the optimization problem and its implementation. In the end, the final shape-optimized design is presented and its performance is validated through several benchmarks, including a comparison with existing one-directional acoustic cloaking designs.

2 BOUNDARY ELEMENT METHOD FOR SCATTERING PROBLEMS

The shape optimization technique is based on the BEM by direct collocation. The formulation of the BEM takes its starting point at the Kirchhoff-Helmholtz integral equation, given by

$$C(P)p = \int_\Gamma \frac{\partial G(R)}{\partial n} p(Q) d\Gamma - \int_\Gamma G(R) \frac{\partial p(Q)}{\partial n} d\Gamma + p^I \quad (1)$$

where p is the acoustic pressure, C is the integral free term, P is a collocation point, Q are integration points on the generator Γ, $G(R)$ is the two dimensional fundamental solution with $R = |P-Q|$ and p^I is an incident pressure. Discretization using collocation and assuming all surfaces to be rigid, i.e. $\partial p/\partial n = 0$, Eq. (1) can be written in matrix form as

$$\mathbf{A}\mathbf{p} + \mathbf{p}^I = 0. \quad (2)$$

The assembly of the **A** matrix is carried out using a MATLAB MEX/C++ compiled boundary element code. the scattered pressure in the domain can be obtained by using field point calculations

$$\mathbf{p}_s = \mathbf{A}_p \mathbf{p}, \quad (3)$$

where $\mathbf{p}_s$ is the scattered pressure at different field points and $\mathbf{A}_p$ is the field point matrix.

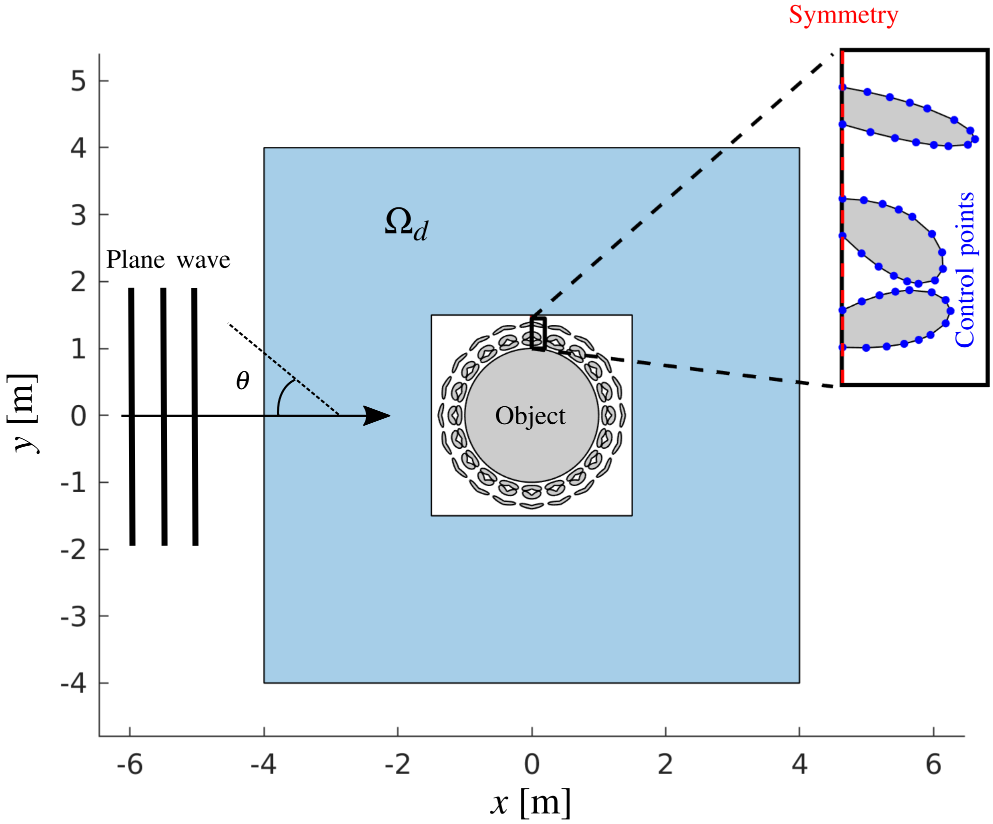

Figure 1. The initial design guess of the multi-directional cloak. The cloak design is based on 3 symmetrically described scatterers that are duplicated every 18 degrees around the cylindrical object, resulting in 20 pairs of identical scatterers. A detailed illustration of the parametrization is seen in the upper right corner, where the blue dots represent the location of the control points that forms the three scatterer pairs. Incident to the design is a plane wave oscillating at 340 Hz with an incident angle of $\theta = 0$. The radius of the cylindrical object is 1 m.

3 INITIAL DESIGN AND PARAMETRIZATION

The initial design guess and the parametrization type are important factors for successful shape optimization. In the case of multi-directional cloaking it is a non-trivial task to guess on a good initial design. The initial guess used here is seen in Figure 1. This design is based on an initial optimization process using the analytical optimization approach found in Ref. [2], where the cloak is described analytically from Bézier scatters and optimized using a combination of a genetic algorithm and simulated annealing [7]. It should be noted that the initial design guess is already an improvement in terms of cloaking of the object.

To conduct the shape optimization the three scatterers are parametrized symmetrically using C^2-continuous parabolic blending to describe the mesh between control points [8]. The locations of the control points are marked by blue dots in Figure 1. The total number of control points is 45 with each control point having the possibility to move in both the x- and y-direction, leading to a total of 90 design variables and a mesh consisting of 5104 quadratic continuous elements. The design of the 3 scatterers is copied for every 18 degrees around the object, meaning that, due to symmetry, the design has 20 possible directions with the same cloaking performance.

4 OPTIMIZATION PROBLEM

The goal is to minimize the scattered pressure in the domain Ω_d (the blue region defined in Figure 1). This is accomplished by solving the optimization problem stated as

$$\begin{aligned} \min_{\mathbf{v}}: \quad & \phi = \int_{\Omega_\mathrm{d}} |\mathrm{p_s}|^2 \, \mathrm{d}\Omega \\ \text{s. t.} \quad & \kappa(\mathbf{v}) - \kappa_{max} \leq 0 \\ & D_{min} - \beta \mathbf{D}(\mathbf{v}) \leq 0. \\ & \text{Eq. (2)}, \end{aligned} \tag{4}$$

where ϕ is the objective function, $\mathbf{v}$ is a vector containing all the design variables, κ is the curvature at each control point, κ_{max} is the maximum curvature allowed, $\mathbf{D}(\mathbf{v})$ is the distance between control points, D_{min} is a minimum allowed distance and β is a self-intersection parameter. A more elaborate description of the curvature and distance constraints can be found in Refs. [5] and [6]. In the following results, $\kappa_{max} = 250$ m^{-1} and $D_{min} = 1.3$ cm. The optimization problem is solved using the gradient-based sequential quadratic programming algorithm in the MATLAB function "fmincon".

4.1 Sensitivity analysis

The gradients with respect to the design variables $\mathbf{v}$ are calculated using a semi-analytical discrete adjoint approach. Therefore, a gradient with respect to a single design variable v can be obtained by [9]

$$\frac{d\phi}{dv} = \frac{\partial \phi}{\partial v} + \Re\left(\lambda^\mathrm{T}\left(\frac{\partial \mathbf{A}}{\partial v} + \mathbf{p}^I\right)\right), \tag{5}$$

here λ are the Lagrange multipliers, which can be found by solving the system

$$\mathbf{A}^\mathrm{T}\lambda = -\left(\frac{\partial \phi}{\partial \mathbf{p}_r} - i\frac{\partial \phi}{\partial \mathbf{p}_i}\right)^\mathrm{T}, \tag{6}$$

where the subscripts r and i denote the real and imaginary parts of the complex pressure. In general, the matrix derivatives are obtained by finite difference at a matrix level using a step length equal to $\sqrt{\text{eps}}$. The sensitivity analysis is performed in parallel using a combination of the MATLAB "parfor" loop and OpenMP.

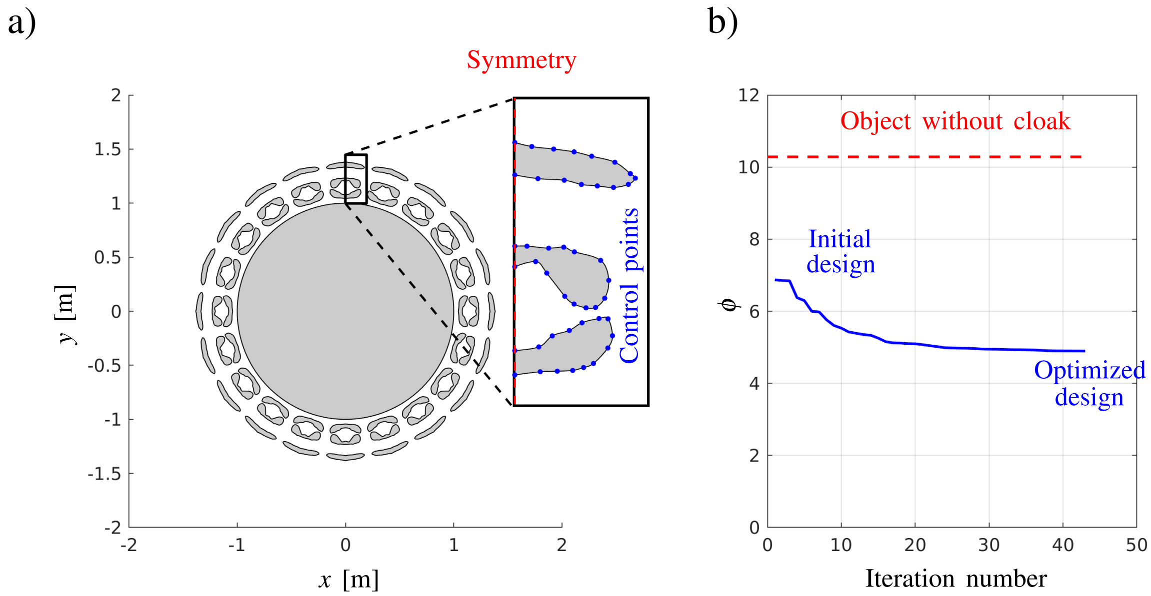

Figure 2. a) Shape-optimized design of the multi-directional cloak, including a magnified area presenting the location of the control points. b) evolution of the objective function ϕ during optimization (continuous blue line). Additionally, the plot includes the value of the objective function when only the cylindrical object is considered (dashed red line).

5 RESULTS

In this section, the results of the shape optimization of the multi-directional cloak are presented. This includes several performance measures studying the frequency dependence, the angle of the incident wave, the effect of viscothermal losses and the visibility of the cloak compared to two existing one-directional cloaking designs. The full optimization time is approximately 3 days and is is performed on a 6 core Xeon E5-1650v3 processor with 128 GB of memory. Figure 2a shows the shapes of the 3 scatterers for the optimized design. The design is very similar to the initial guess, indicating that the initial design is very important for the shape optimization outcome. In Figure 2b, the evolution of the objective function for each iteration is shown. Aditionally, the figure also includes the objective function when only the cylindrical object is considered. The optimized design is an improvement over the initial guess, with a value of the objective function around $\phi = 4.9$, lower than in the initial design ($\phi = 6.8$). However, the design does not achieve an objective function close to zero, which would correspond to perfect cloaking and complete reconstruction of the incident wave.

5.1 Cloak performance as a function of the incident angle and frequency

The objective function with respect to the frequency of the incident wave is plotted in Figure 3a. As expected, the optimized design reduces the objective function at the optimization frequency. Additionally, the optimized design shows a better "broadband" performance as compared to the initial design. It should be noted, that this broadening of the response is obtained using a single optimization frequency and it is not included as an optimization criterion.

Moreover, Figure 3b shows how the objective function of the initial and optimized designs depended on the incident angle of the impinging plane wave. The incident angle has very little influence on the cloaking performance. Figure 3a and Figure 3b also includes comparative Finite Element Method (FEM) simulations of the optimized design. The FEM simulations are performed using COMSOL Multiphysics.

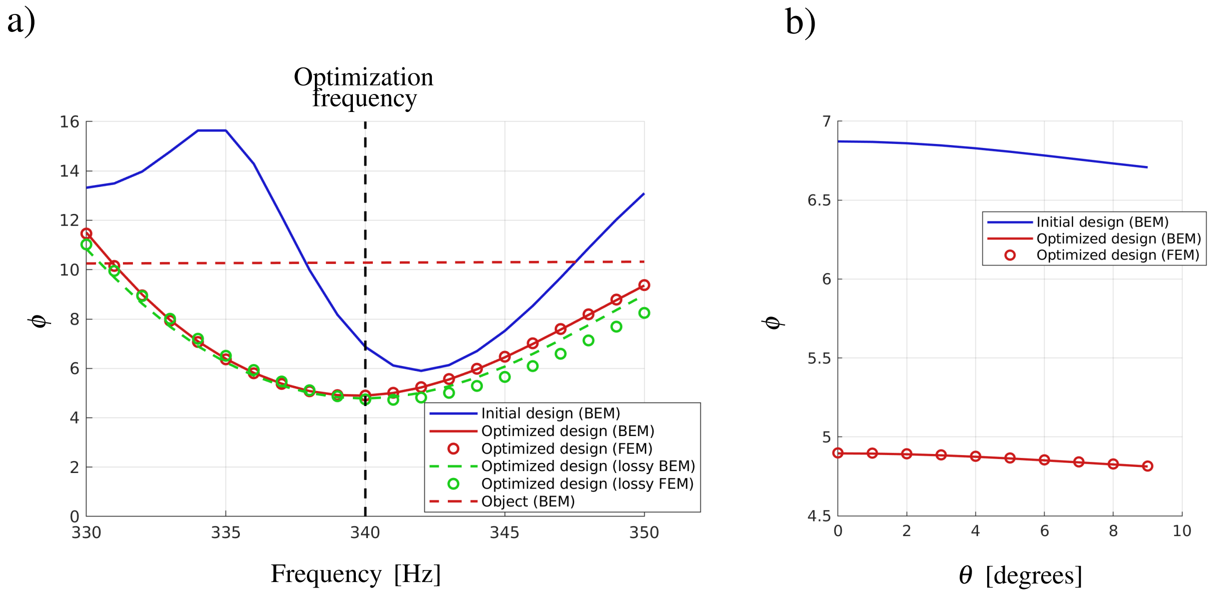

Figure 3. a) Frequency dependence of the objective function for both the initial (blue) and the optimized (red) design. The figure also includes simulations including viscous and thermal losses (green). b) Dependence of the incident angle of the impinging plane wave for the initial (blue) and the optimized (red) design. circular symbols represent equivalent FEM simulations for comparison.

5.2 Effect of viscous and thermal dissipation

The effect of viscous and thermal dissipation on acoustic cloaks based on scattering cancellation was previously studied in Ref. [10]. In this reference, it is concluded that the effect of viscothermal losses can be neglected when performing simulations on cloaking devices. However, since the design proposed here is fundamentally different from the designs found in Refs. [1, 2, 6], with much more compactly arranged scatterers, a study of the effect of losses on the objective function seems appropriate. Therefore, the frequency dependent behavior of the objective function is also plotted in Figure 3a for both full viscothermal BEM and FEM simulations (green curves). The lossy BEM simulations are based on the Kirchhoff decomposition of the full linearized Navier-Stokes (FLNS) equations and implemented following the approach in Ref. [5]. On the other hand, the FEM simulations are carried out using the FLNS implementation in COMSOL Multiphysics. It is observed that the effect of losses on the objective function is small, and simulations of the objective function are very similar to the isentropic computations. However, small discrepancies between the two lossy BEM and FEM simulations can be observed. A possible explanation for the discrepancies might be due to differences in their mesh densities. The lossy FEM simulations are performed using a mesh with approximately 8 million degrees of freedom. On the contrary, the BEM calculations are based on the same mesh as the isentropic BEM calculations. Similar small discrepancies between viscothermal FEM and BEM calculations are found in Ref. [10].

5.3 Visibility comparison with existing one-directional cloaks

A common measure to validate the cloaking performance is the so-called average visibility. The definition of the average visibility and how to calculate it can be found in, e.g., the Refs. [1, 10]. In Figure 4, the average visibility of the shape-optimized multi-directional cloak is plotted and compared to two one-directional cloaks that can be found in Refs. [1] and [6]. The two one-directional cloaks are either created using a distribution of 120 cylinders or using shape optimized scatterers based on the same approach used in this paper. The cloaks are designed with different operational frequencies in mind. Therefore, the frequency behavior is normalized with respect to their individual operational frequency f_0. As expected, the visibility of the multi-directional cloak is not as low as for the cloaks optimized for a single direction.

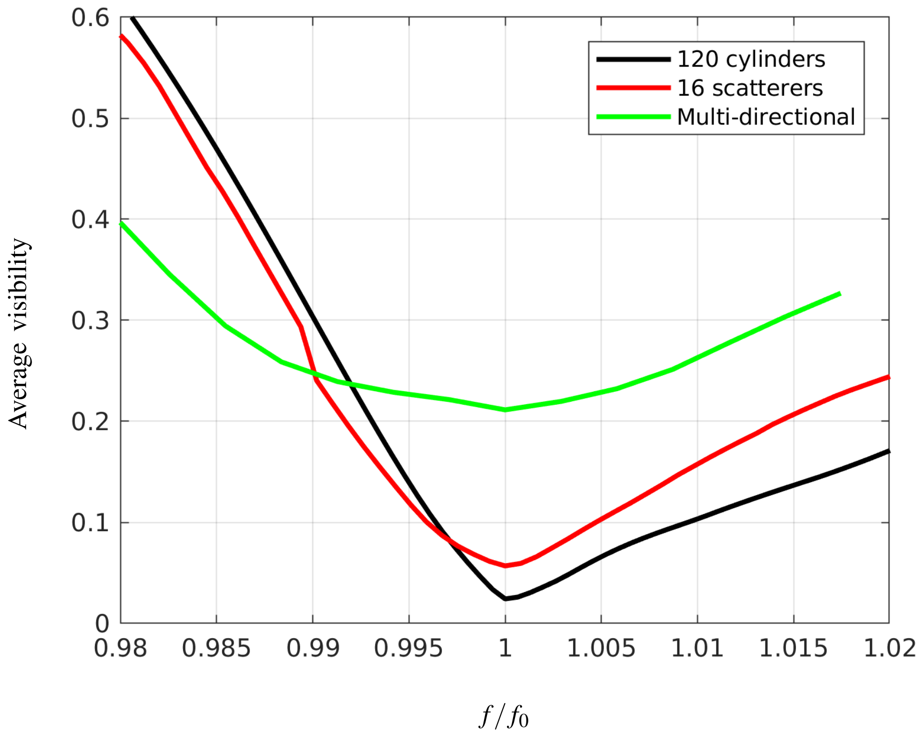

Figure 4. The visibility of the optimized multi-directional cloak compared to two one-dimensional cloaks found in the literature. The black curve is the visibility of the cloak found in Ref. [1] which consists of 120 cylinders, and the red curve is the visibility of the shape-optimized one-dimensional cloak found in Ref. [6]. The green curve represents the visibility of the shape optimized multi-directional cloak as seen in Figure 2a. Here, the frequency f is normalized with respect to the operational frequency of the different cloaks. The operational frequency is denoted by f_0.

6 CONCLUSIONS

In this work, a newly developed shape optimization technique has been utilized to improve the design of a multi-directional cloak based on Bézier scatterers. Although the shape-optimized multi-directional cloak is out performed by the one-directional cloaks at the design frequency, it offer a broader frequency range of operation, also compared with the initial omni-directional design. Interestingly, the proposed design is very robust with respect to the angle of the plane wave (Figure 3b). In fact, the cloaking performance does not depend on the incident angle making the design truly omni-directional.

The shape optimization results presented here should be considered an initial step towards creating high-performing multi-directional acoustic cloaking devices. Several measures can be taken to improve on the optimized design by, e.g., adding more scatterers or altering the initial location of the scatters, and perhaps including the location of the scatter as additional design variables. Moreover, optimization studies can be performed with less restrictive constraints on, e.g., the curvature κ. This would allow for more design freedom perhaps improving the cloaking performance. The negligible angle dependence of the optimized cloak suggests that the periodic scatterers could be made broader and fewer. It can also be concluded that, even though the scatterers of the initial and optimized designs are compactly arranged, the dissipative effects can safely be neglected in the optimization procedure.

ACKNOWLEDGEMENTS

J. Sánchez-Dehesa acknowledges the support by the Spanish Ministerio de Economıá y Competitividad, and the European Union Fondo Europeo de Desarrollo Regional (FEDER) through Project No. TEC2014-53088-C3-1-R.

REFERENCES

[1] García-Chocano,V. M.; Sanchis L.; Díaz-Rubio, A.; Martínez-Pastor, J.; Cervena, F.; Llopis-Pontiveros, R.; Sánchez-Dehesa, J. Acoustic cloak for airborne sound by inverse design. Applied Physics Letters, 99 (7), 2011, 074102

[2] Lu, Z.; Sanchis L.; Wen J.; Cai L.; Bi,Y.; Sánchez-Dehesa, J. Acoustic cloak based on Bézier scatterers. Scientific Reports, 8 (1), 2018, 12924

[3] Andkjær, J.; Sigmund, O. Topology optimized cloak for airborne sound. ASME J. Vib. Acoust., 135, 2013, 041011.

[4] Jo, C.; Jeong, J.; Kwon B.; Park, K.; Oh, I. Omnidirectional two-dimensional acoustic cloak by axisymmetric cylindrical lattices. Wave Motion, 54 , 2015, 157-169.

[5] Risby Andersen, P.; Cutanda Henríquez, V.; Aage, N. Shape optimization of micro-acoustic devices including viscous and thermal losses. Journal of Sound and Vibration, 447, 2019, 120-136.

[6] Risby Andersen, P. Modelling of acoustic viscothermal losses using the Boundary Element Method: From method to optimization. PhD thesis, The Technical University of Denmark, Lyngby, Denmark, 2019

[7] Sanchis, L., Cryan, M. J., Pozo, J., Craddock, I. J.; Rarity, J. G. Ultra high Purcell factor in photonic crystal slab microcavities. Phys. Rev. B, 76 , 2007, 157-169.

[8] Johnston, P. R. C2-continous elements for boundary element analysis. International Journal for Numerical Methods in Engineering, 40 , 1997, 2087-2108.

[9] Dühring, M. B.; Jensen, J. S.; Sigmund, O. Acoustic design by topology optimization. Journal of Sound and Vibration, 317 , 2008, 557-575.

[10] Risby Andersen, P.; Cutanda Henríquez, V.; Aage, N. Sánchez-Dehesa, J.; Visco-thermal effects on an acoustic cloak based on scattering cancellation, Proceedings of NOise and Vibration Emerging Methods, Ibiza, Spain, 2018